

The Rise and Fall of Baryons

Shu Lin and Edward Shuryak

Department of Physics and Astronomy, Stony Brook University, Stony Brook NY 11794-3800, USA
(Dated: May 31, 2019)

We discuss the baryonic contribution to QCD thermodynamics near the QCD phase transition, which we split into “stringy excitations” and the “chiral” lowest states. Our finite- T string model for the former component is inspired by the lattice data on static potentials and ideas of string survival even *above* T_c : it is used to explain two sets of baryonic susceptibilities calculated on the lattice by the Bielefeld-BNL group. Two new ingredients of the model are (i) the near- T_c tightening of the strings, and (ii) physical upper limit of the string length. Then we proceed to more subtle effects related to chiral restoration dynamics near T_c : we suggest that “melting” of the sigma terms of the lowest nucleon/ Δ masses can explain these susceptibilities. In a discussion, we consider bound monopole-quark states, as a possible explanation to some deficits of contribution at $T = (1 - 1.4)T_c$.

PACS numbers:

I. INTRODUCTION

The issues discussed in this paper deal specifically with the sector of the QCD states with a nonzero baryonic charge, the *baryons* in the confining phase and *quarks* in the deconfined one. They are however part of a more general discussion about the fate of hadronic states near and above the deconfinement phase transition.

Hadronic spectroscopy study the lowest hadronic states in great details: but as the excitation energy grows the task of exact quantum number identification gets more challenging. Eventually the decay widths of the hadrons becomes comparable to distances between the states, or exceeds it $\Gamma > |E_i - E_j|$: here identification of the individual states becomes impossible. Yet it does not mean that the states (and their density) do not exist: multiple examples from other fields of physics – e.g. the overlapping neutron resonances in nuclear physics – show that. The thermodynamical quantities are averaged over all states excited at some well defined conditions, and those include the states which we cannot identify individually. We need certain models about hadronic states at one hand, to understand/reproduce the available (lattice) results on the thermodynamics: this is the main logical direction of this paper.

While the temperature and the baryonic chemical potential are small $T, \mu \ll T_c$, hadronic matter is a dilute gas of basic hadrons, e.g. pions and nucleons, and thermodynamics must be given by elementary ideal gas formulae, plus interaction corrections given by the standard virial expansion. As one approaches T_c from below, many excited states of basic hadrons come into play, and hadrons become more densely packed and more strongly interacting. It is widely believed that a consistent treatment of this matter is given by a “resonance gas” approximation, in which interaction is taken care of by counting all resonances on equal footing with stable hadrons[1]. Furthermore, when the vicinity of the critical region is reached $T \sim T_c = 170 - 190 \text{ MeV}$, new phenomenon (referred to as “*rise*” in the title) happens, in which ther-

modynamical quantities grow by about an order of magnitude in a rather narrow interval of temperatures.

Statistical bootstrap model (hadrons are bags made of other bags) lead Hagedorn in 1960’s to the conclusion that the density of hadronic states $\rho(m)$ may grow exponentially with the mass m . If this be the case, Hagedorn argued, at some temperature this growth would be cancelling the Boltzmann exponent, preventing hadronic systems from being heated to temperatures above it. Thus he predicted certain *maximal possible temperature* in Nature, $T < T_{\text{Hagedorn}}$ [2]. The development of QCD in 1973 has lead to the opposite conclusion: the high- T phase of QCD is in fact the so called *quark-gluon plasma* (QGP) [3] in which the density of states grows like the power of the mass, like for other “normal” systems. Later, Hagedorn reinterpreted his argument as the maximal possible temperature of the *hadronic phase*, taking it as an early indication to the existence of the QCD deconfinement phase transition. The basic physics of Hagedorn phenomena was explained by Polyakov and Susskind in 1970’s who pointed out that exponential growth of the density of states is the natural consequence of the QCD string model.

As T gets higher than T_c , hadronic (e.g. baryonic) contribution to thermodynamics gets replaced by free quarks and gluons.. The issues we will be discussing in this paper is what exactly happens in the so called “RHIC domain”, $T = (1 - 2)T_c$. As we will see, lattice susceptibilities tell us that the rapid rise of hadronic states changes to nearly equally rapid *fall*, at $T \sim 1.1T_c$: there is no consensus about its exact physical nature. This question will in turn lead us to the issue of whether the very existence of strings above T_c is or is not possible. Our point of view is that not only it is, but recent RHIC discovery of the so called “soft ridge” shows existence of quite robust strings, surviving for several fm/c such conditions, for related discussion see [4]. We also would claim that “stringy” excitations dominate the rise and the fall of the baryonic excitations: the latter related to the increase of quark density and shortening of the *mean* length of the

strings.

In order to discuss these issues and provide some (model dependent) answers to those and many similar questions we had selected a particular subset of hadrons, namely the *baryons*. The reason for that is that by considering susceptibilities – the quantities obtained by certain number of derivatives over the baryonic chemical potential μ – we insulate the issue from much more complicated sector of states with *zero* baryon number, including mesons, glueballs or even more exotic quasiparticles such as monopoles/dyons.

The inputs to our study is provided by the lattice data sets from two papers, by UK-Bielefeld-BNL group, to be referred below as the Set 1 and Set 2, respectively. The former one [5] is for $N_f = 2$, two quark flavors with a rather heavy pion mass, $m_\pi \approx 770 \text{ MeV}$. The latter is a more recent work [6] is closer to the real world, it includes the strange quark and also has much smaller pion mass $m_\pi \approx 220 \text{ MeV}$. (Unfortunately, the latter one has also somewhat larger fluctuations and thus error bars.) Since those two sets correspond to two different worlds, all quantities in question – including the baryon masses and the critical temperatures themselves – are different, and reproduction of their differences would be one of the tasks for our model to reproduce.

The most prominent feature of these susceptibilities are illustrated in Fig.1, which shows the ratio of the 4-th to the second derivative over baryon chemical potential, to be called *kurtosis* for brevity. One can see from this figure that the kurtosis drops rapidly from 9 to 1 as the temperature crosses T_c . It finds a very simple explanation: while the baryonic partition function is proportional to $\cosh(3\mu/T)$, that of quarks has just $\cosh(\mu/T)$, and two derivatives of those functions explain 9 and 1 in the corresponding phases. This means that the confined phase is dominated by baryons and the deconfined one by quarks.

While this conclusion is basically correct, a detailed study of these transition and the T -dependence of the susceptibilities will reveal many more interesting details of the transition. The susceptibility d_4 in particular show a very dramatic rise at T_c , complemented by a rapid drop right after that. Both these features are driven by the baryon sector, and not by the quarks – as we emphasized by the title of the paper. The reason for this to happen, as well as some model describing it, is the main part of this paper.

Physics related to these data has been discussed by Liao and Shuryak [7], who emphasized the presence of at least the lowest baryons in the region of $T = (1 - 1.4)T_c$, and in particular the T, μ -dependence of their masses. It was based on a previous paper by the same authors [8] in which lattice-based potentials between quarks were used to study when quark quasiparticles can form bound states. From a variational solution to the 3-quark Schrödinger equation they concluded that only the lowest states should survive, remaining bound in the T interval just mentioned. Another issue is whether the baryon and

quark effective masses are μ -dependent. If they are, that generates deviations from 9 and 1 in the kurtosis, and certain changes in the susceptibilities: as we will show below, those compare well with the latest lattice data. In our discussion below we will separate those lowest states from “stringy” excitations.

Weise and collaborators [9, 10, 11] have provided very descriptions of these data in the PNJL model: their main idea was that the single quark and diquark contributions are both suppressed close to T_c by small VEV of the Polyakov loop $\langle L(T) \rangle$. Although this model has no baryons per se, only the colorless combinations of three quarks (so to say, “proto-baryons”) are the colorless states which are not suppressed by the Polyakov loop in the near- T_c region, and is thus the main contributor to thermodynamics there.

Finally, there are two more important physics issues, both related to the chiral dynamics. The first is the dependence of baryonic susceptibilities (and of course masses) on the value of the light quark mass m_q in the theory. It has been studied a lot by the lattice community, but in the vacuum (at $T = 0$) rather than not at $T \approx T_c$. The derivative of the baryon mass over the quark mass – known as the “sigma term” – is a chirally odd quantity, expected to vanish at $T > T_c$ in the chiral restoration transition. So, we will be look for observable consequences of that, in the lattice data set under consideration.

The paper is structured as follows. Section II is devoted to “stringy excitations” of baryons, in it we develop a somewhat modernize model of the phenomenon, which goes back to Polyakov-Susskind excitation of strings. We will show that this phenomenon can indeed naturally describe very rapid rise in baryonic contribution to thermodynamics near T_c . We have also added a restriction on the upper limit of the string length related to quark density: this turns out to produce the observed “fall” of the stringy baryons. The density of quarks in the near- T_c region is calculated with recent lattice data on quark effective masses as well as Polyakov loop, see section III. In section IV we subtract the quark gas contribution from all susceptibilities and compare it to our model calculation for “stringy” and “non-stringy” baryons. Effects of chiral dynamics, which determine m_q , T and μ dependencies of the baryon mass, are discussed in section V. Discussion of some open issues is placed in section VI: one of them is the role of bound states between quarks and magnetic objects, monopoles/dyons, which (to our knowledge) are discussed in the QGP context for the first time. We present some crude estimates of their possible contribution, and find that it seems to be of the same magnitude as “unaccountable” contribution with quarks and baryons.

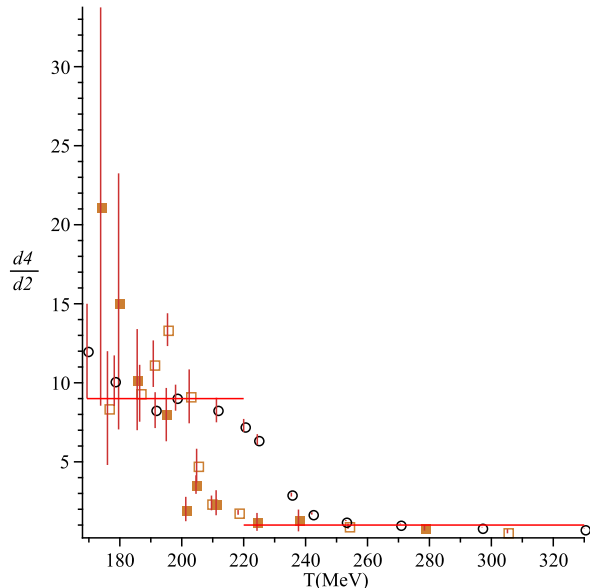


FIG. 1: (Color online) The temperature dependence of the “kurtosis”, the ratio of susceptibilities d_4/d_2 . The Set 1 (2 flavor QCD at $m_\pi = 770$ MeV) are shown by black circles, while Set 2 (2+1 flavor QCD at $m_\pi = 220$ MeV) is shown by (brown) solid boxes for $N_\tau = 6$ and open boxes for $N_\tau = 4$. The upper and lower horizontal lines correspond to the values 9 and 1, respectively.

II. STRINGY BARYONS

A. Hagedorn transition and the string model

Specific realization of Hagedorn’s ideas came with the advent of the QCD strings. Let us briefly remind this well known argument here, for introduction of notations. An important parameter of the string a , to be referred to as “the string scale”, is loosely speaking a length of the string section which can be moved independent from other segments. (This loose idea implies that it should be some $O(1)$ number times the string width.) Its precise definition is given in terms of the number of string states. Suppose a string has certain length L and tension σ , so its energy is $E = \sigma L$.

$$\rho(L) \sim \exp(S(L)) \sim 5^{L/a} \quad (1)$$

Here $5=2d-1$ is the number of directions the string may turn to in d -dimensional space without self-crossing, after a segment of length equal to a . Now, combining the entropy and energy together one gets stringy partition function in the generic form

$$Z_{string} = \int dL e^{\ln(5)L/a - \sigma L/T} \quad (2)$$

which diverges as the temperature approaches the Hagedorn critical temperature

$$T_c = \sigma a / \ln(5) \quad (3)$$

Note that at this temperature the exponent (the free energy of the string $F = E - TS$) goes to zero, allowing the string to get arbitrarily long.

Now, does this simple string model describe properties of the deconfinement transition observed on the lattice, for various gauge theories?

Before answering this question, one needs to specify the string scale scaling. The string tension scales as

$$\sigma \sim E^2 a^2 \quad (4)$$

if E is the electric field strength and a is the string width. At the same time the electric flux, which should match the electric charge at the end of the string, is $flux = Ea^2 = const$, from which one concludes that the scaling must be

$$\sigma \sim E \sim 1/a^2 \quad (5)$$

Using this argument one expects that $T_c/\sqrt{\sigma}$ should be some universal constants: and in fact for pure gauge theories with different number of colors N_c this prediction actually works well for large N_c , see e.g. [12].

For readers who are not simply satisfied by the scaling of T_c and are unsure if the deconfinement is the string Hagedorn transition, it is instructive to look at lattice measurements of the string free energy. Such measurements, for N_c as large as 12 has been made by Bringoltz and Teper [12]: see one of their figures is reproduced in Fig.2. As one can see from it, with increasing T the effective (free energy) tension is indeed decreasing, roughly linearly: this would agree with the idea that the energy of the string is hardly affected by the temperature and the decrease is due to T times the entropy of string states. However at $T/T_c = 1$ the free energy tension is *not* zero but only about half of the vacuum value: using metastability of the 1-st order transition the authors were able to extend the curve about 5% above T_c and show that the trend continues: the projected Hagedorn temperature is perhaps $T_H = 1.11T_c$ or so. Thus, the deconfinement at large N_c is *not* the Hagedorn transition, although it scales similarly and is numerically close to it.

B. Strings at finite temperatures in QCD-like theories with quarks

QCD with the physical quark masses is different from all large N_c pure gauge theories because instead of the first order transition with a large jump one has instead rather continuous “crossover” transition. The continuity of the transition allows us to ask if any role is played in the QCD phase transition by the Polyakov-Susskind string argument outlined above, at and above T_c .

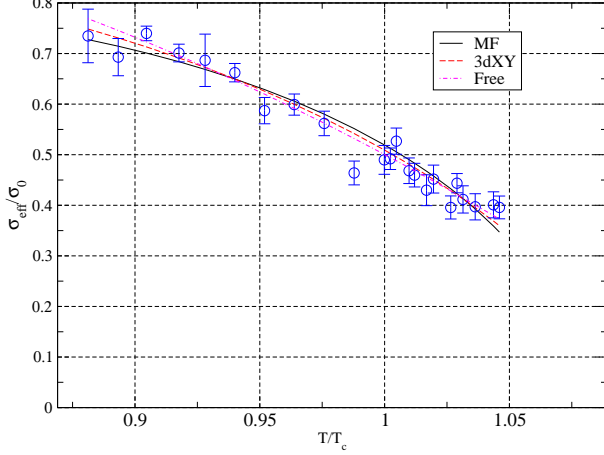


FIG. 2: (Color online) Temperature dependence of the free energy tension σ_F , for the SU(10) gauge theory according to Ref.[12]

Before we start answering this question, let us first review what is known about QCD strings, at zero and finite- T , *microscopically*. At $T = 0$ there are extensive lattice studies of string tension, shape, internal structure [13] and even the string breaking [14]. It is done by inserting two static charges and studying their influence on the gauge fields: it helps by the fact that at $T = 0$ the string is just straight, with small influence of quantum vibrations. We will not go into details here, just mention that the shape fits well into the “dual superconductor” picture, with condensed monopoles creating a coil of magnetic current around it. The distribution of the electric field fits well into the solution of (dual) Maxwell equations in superconductor found by Abrikosov

$$E(r) \sim K_0(r/\lambda) \quad (6)$$

with the length parameter $\lambda \approx .15 fm \approx (1.3 GeV)^{-1}$ [13]. Unfortunately, at finite T thermal fluctuations of the string make such studies much more challenging, and so we do not have similar results in the near- T_c region.

Yet there are still extensive lattice studies of the thermodynamical quantities associated with a pair of two stationary $\bar{q}q$ [15, 16]. We will not review this large subject here, but only comment on the *linear* (in distance) part of these static potentials. Let us define the free energy tension $\sigma_F(T)$ and entropy tension $\sigma_S(T)$ as follows

$$V = \sigma_V(T)L + V_0 \quad (7)$$

$$F = \sigma_V(T)L + V_0 \quad (8)$$

$$S = \sigma_S(T)L \quad (9)$$

where V_0 is a constant. Standard thermodynamical relations $U = F + TS$, $S = -dF/dT$ imply the same relations

for tensions

$$\sigma_V = \sigma_F + T\sigma_S \quad (10)$$

$$\sigma_S = -d\sigma_F/dT \quad (11)$$

The free energy(entropy) string tension, and the string scale are obtained by solving (10) with the string tension of the potential energy as the input. We obtained:

$$\sigma_F = -T \int_{T_0}^T \frac{\sigma_V(T)}{T^2} \quad (12)$$

The constant T_0 will be fixed at the end of this section as $0.95T_c$. In Fig.(3) we show the input string tension of the potential energy and the resultant free energy string tension. The input are lattice σ_V extracted from lattice work [15] parametrized by:

$$\frac{\sigma_V}{T_c^2} = 26.21e^{(-11.40\sqrt{(T/T_c-1)^2+6.78\times 10^{-4}})} + 4.76. \quad (13)$$

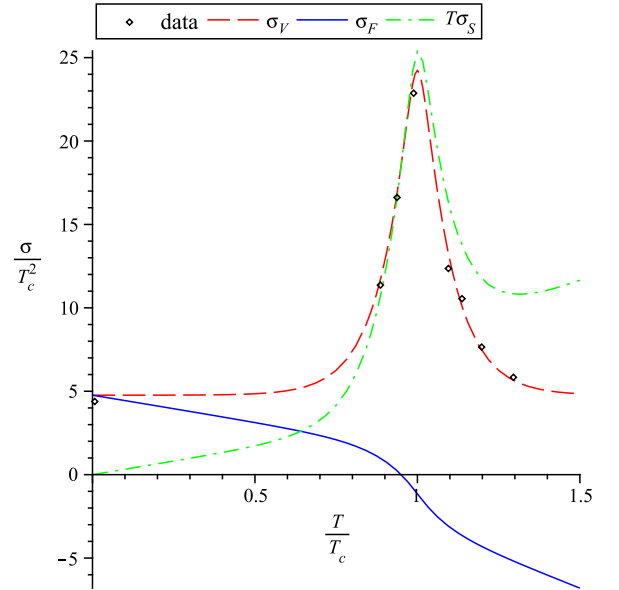


FIG. 3: (Color online) The temperature dependence of two string tensions, σ_V (red dashed line), σ_F (blue solid line). The entropy term $T\sigma_S$ is shown by the (green) dash-dotted line. The lattice data points shown are for σ_V extracted from lattice work [15].

C. T-dependent string model and density of states

One can build a simple model based on the same number of state as for the fundamental string. Suppose T -dependent string scale $a(T)$ be known: then we postulate the density of states to be

$$\rho(L) \sim 5^{L/a(T)} = e^{\sigma_S(T)L} \quad (14)$$

but now with effective T -dependent string scale. To write the density of states per unit mass, we note $m = m_0 + \sigma_V(T)L(T)$, with m_0 the contribution from the quark ends. As the string tension $\sigma_V(T)$ changes with temperature, the string length $L(T)$ corresponds to certain baryon state changes qualitatively in the opposite way, i.e. a tight string is short in length. In this paper, we simply assume the combination $\sigma_V(T)L(T)$ remains constant. The string inspired density of states is given by:

$$\rho(m) = ce^{\sigma_S(T)L} = ce^{\sigma_S(T)/\sigma_V(T)(m-m_0)} \quad (15)$$

The normalization constant c in (15) and T_0 in $\sigma_S(T)$ will be fixed by matching the experimental data at $T = 0$.

In order to make comparisons with the output of lattice simulation, where large unphysical quark masses are used. We adopt the following expression for the baryon masses:

$$m_B = \sigma_V(T)L(T) + N_s m_s + km_\pi^2 \quad (16)$$

in which the first string term is complemented by two more terms, which describe the dependence of the “string’s ends” on the strange and light quark masses. (This is needed because the comparison is done with various data sets using unphysical quark mass used in lattice studies.)

The second term is just additive dependence on the strange quark mass, with N_s the number of strange quarks in the baryon. The light quark mass (pion mass) dependence is included via the *slope*

$$k = \frac{\partial m_B}{\partial m_\pi^2} \quad (17)$$

known also as a “sigma term”. It depends nontrivially on the baryon in question, see lattice studies such as [17]. The N and Δ channels have stronger dependence than the Λ and Σ channels, which contain more strange quarks. We list the slope k extracted from [17] for relevant channel in Tab.I. The Ω channel contains only strange quarks, therefore we assume the slope to be zero. Note the lowest states of each channel is separated from the other resonances by a significant gap, and they have different properties (we will call them “chiral baryons” and further justify this separation in section V). These lowest states (for three flavors the 56-plet, spin 1/2 octet $N(938), \Lambda(1116), \Sigma(1195), \Xi(1317)$ and 3/2 decuplet $\Delta(1232), \Sigma^*(1385), \Xi^*(1530), \Omega(1672)$ f or its subset for two flavors) are treated separately from the rest of “stringy” (also called hybrid) excitations.

Let us return to the density of states of “stringy excitations”, by which we count all resonances to which, for

TABLE I: slope k for different channels

$N(GeV^{-1})$	$\Delta(GeV^{-1})$	$\Lambda(GeV^{-1})$	$\Sigma(GeV^{-1})$	$\Xi(GeV^{-1})$
0.79	0.73	0.61	0.55	0.3

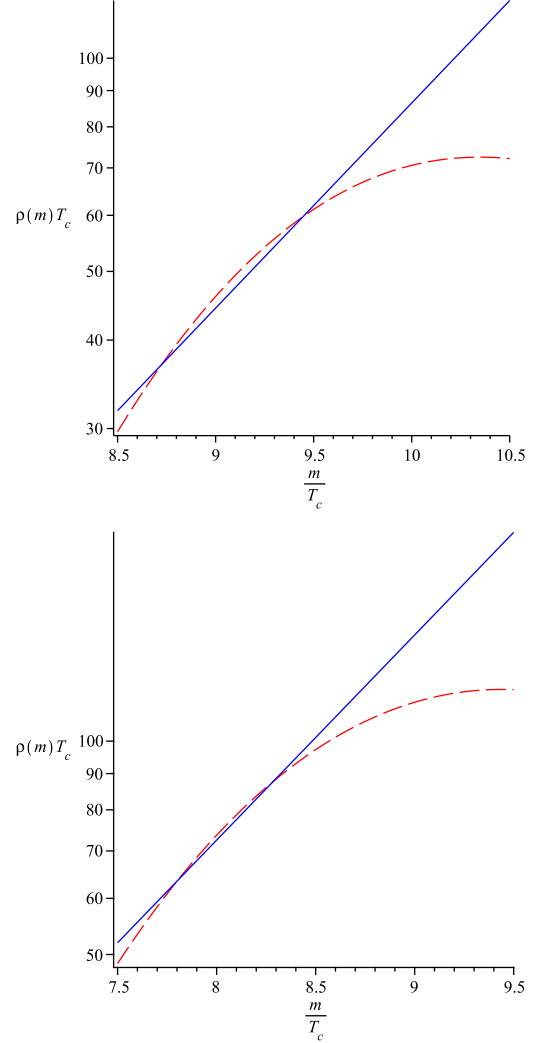


FIG. 4: (Color online) The “string inspired” exponential fit to the baryonic density of states, for Set 1 and Set 2 (upper and lower figure, respectively). The (red) dashed line is the sum of over all resonances listed in Particle Data Book [18], with masses corrected to lattice quark mass by expression(16). The (blue) solid line is the exponential fit: $\rho(m) = 0.11e^{m/1.5}$ (Set 1) and $\rho(m) = 0.35e^{m/1.5}$ (Set 2), with unit set properly by T_c .

smoothness we assign a width of $200MeV$. We modify the baryonic resonances according to (16) and fit the density of states by the string inspired exponential function (15). Fig.4 shows the exponential fitting to the densities of states.

Comparing our string model predictions with lattice

thermodynamics we will have the following parametrizations for $N_f = 2$ $c = 0.11e^{m_0/1.5}$ (Set 1) and $N_f = 3$ $c = 0.35e^{m_0/1.5}$ (Set 2). Furthermore the parameter T_0 in (12) is fixed by the requirement $\sigma_S/\sigma_V = 1/1.5T_c^{-1}$ at $T = 0$, thus $T_0 = 0.95T_c$. It is important to note the critical temperature corresponding to Set 1(2 flavors at $m_\pi = 770MeV$) and Set 2(2+1 flavors at $m_\pi = 220MeV$) are slightly different. The former has $T_c = 220MeV$, while the latter has $T_c = 200MeV$ (They can be obtained from [19, 20]). Special attention should be paid in converting the absolute unit to units of T_c , different for each set.

III. QUARKS IN THE NEAR- T_c REGION

We postulate that the free energy (pressure) due to quarks and antiquarks is given by the usual free gas formula

$$p_q(T, \mu = 0) = d \frac{1}{\pi^2} m_q^2 T K_2(m_q/T) \cosh(\mu/T) \langle L(T) \rangle \quad (18)$$

modified by the last factor, the so called the Polyakov loop,

$$\langle L \rangle = \frac{1}{N_c} Tr \left[\mathcal{P} e^{ig \int d\tau A_0(x)} \right] \quad (19)$$

induced by the presence of nonzero A_0 gauge fields. The corresponding lattice data and our parametrization of both the assumed quark effective mass and the Polyakov factor are described in the Appendix.

As those calculations are rather standard, we would not show the quark contribution itself, showing in several plots below only the susceptibilities with and *without* quark contribution, shown by boxes and circles, respectively. The latter contributions show a near- T_c peak and then decrease, disappearing around $1.5T_c$. Our task in the section to follow would be the interpretation of these “non-free-quark” contributions.

A. Quarks restrict the string length

As this and similar examples show, one has inevitably $\sigma_F(T)$ crossing zero. We would however argue that unlike in the string-Hagedorn transition, the string length should not be allowed to become indefinitely large and the partition function to diverge. The reason for that is string breaking/flipping. Let us introduce the *quark scale*

$$L_q(T) = n_q^{-1/3} \quad (20)$$

related to their density in the QCD matter at temperature T .

Note the quark density n_q from naive derivative of the quark pressure with respect to μ will give $\sinh(\mu/T)$, which vanishes at $\mu = 0$ due to the cancellation between quarks and antiquarks. We instead use $\cosh(\mu/T)$, as

both quark and antiquark can be the end points of a string. It is also required by the $\mu \leftrightarrow -\mu$ symmetry. The degeneracy factor $d = 2(2S+1)N_c N_f$. Suppose we start with a string, whose ends are fixed, for simplicity at some nearby points. If the string length is L and its shape is random, the average distance from the original ends would be given by random walk expression

$$\langle (\delta x)^2 \rangle \sim a^2 (L/a) \quad (21)$$

where L/a is the number of random turns. We will then argue that as a string reaches the “domain of influence” of other quarks, the string would not grow anymore in length but get switched to another quark. We thus postulate that

$$\langle (\delta x)^2 \rangle \sim a^2 (L/a) < L_q^2 \quad (22)$$

sets the upper limit in the integral over the string length:

$$L_{max} = y^2 L_q^2 / a \quad (23)$$

with y is some constant of order 1. Correspondingly, $m_{max} = m_0 + \sigma_V(T) L_{max}$. The temperature dependence of L_q is such that at $T < T_c$ it is very large, reaching large but finite at T_c , and then rapidly decreasing.

We compare various length scale appearing in the model in Fig.5. At temperature $T \sim 0.8T_c$, the string length can get very long, but long strings are suppressed by Boltzmann factor. As the temperature crosses the critical value, the density of states starts to win over the Boltzmann factor and the string length cutoff becomes important, as illustrated by the dropping of the L_{max} near T_c . At $T \sim 1.1T_c$, the stringy baryon picture breaks down as $L_{max} \sim a$.

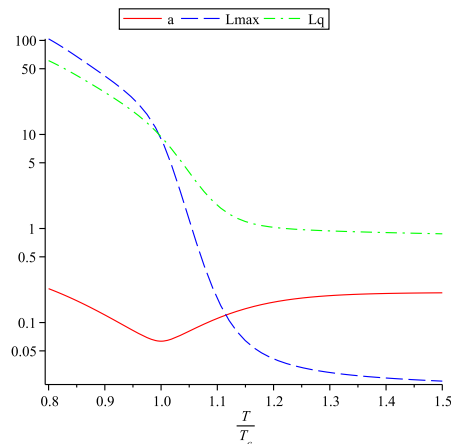


FIG. 5: (Color online) A comparison of the string length cutoff L_{max} (blue dashed line) and string scale a (red solid line) at different temperatures for two flavors QCD. L_q (green dash-dotted line) is also included for comparison. The parameters used in the plot is $y = 0.08$, $T_0 = 0.95T_c$

IV. THERMODYNAMICS OF THE “STRINGY BARYONS” IN THE NEAR- T_c REGION

Now we collect all the pieces of our string-inspired model and calculate several susceptibilities $d_n(T)$, to be compared with Set 1 and 2 lattice data. On the string side, the most important aspects are the “string tightening” in the near T_c region, as well as the free energy tension crossing zero and creating elongation of the string. With the string tension σ_V extracted from lattice potential, we obtained σ_F and σ_S from (12) and (10), which allows us to determine the density of states. The latter can be used to calculate the pressure and susceptibilities. Here, for the record, are their definitions

$$p(T, \mu) \equiv \frac{T \partial \ln Z(T, \mu)}{\partial V} = \sum_i \frac{1}{\pi^2} \frac{m_i^2}{T^2} K_2(m_i/T) + \int_{m_{min}}^{m_{max}} \frac{1}{\pi^2} \frac{m^2}{T^2} K_2(m/T) \rho(m) dm \quad (24)$$

$$d_n(T) = \frac{\partial^n (p/T^4)}{\partial (\mu/T)^n} \Big|_{\mu=0} \quad (25)$$

The lowest states counted separately by the index i include the 20-plet of N, Δ for $N_f = 2$ or the members of the 56-plet, if the strange quark is present. The second term is the contribution from the continuum assumed to be stringy excitations. The upper bound in integration is given by $m_{max} = m_0 + \sigma_V(T) L_{max}$ and the lower bound m_{min} is given by the mass of the first excited state in N channel, with unphysical quark mass properly taken into account by (16).

Now is the time to show the results and confront it with lattice findings on susceptibilities. We show those, with and without the free quark contribution, in Fig.6 for the first susceptibility d_2 .

The red dashed line show the contribution of the “stringy” baryons, while the dash-dotted line show the contribution of the lowest “chiral” states. First of all, the stringy states, albeit higher in mass, predominates over the lowest states near T_c , and their rise explains the data, both in magnitude and in the growth rate. Their dominance is more prominent at larger bare quark mass (Set 1) than at smaller bare quark mass (Set 2), the latter having smaller masses for the lowest states. Another reason why Set 2 has larger contribution of the non-stringy baryons is that it has $N_f = 2 + 1$ rather than 2, which causing further proliferation of baryons relative to quarks.

As the temperature rises above T_c , the string model predicts the fall of the baryons caused by quark proliferation and a decrease of the string length. It happens when $m_{min} \sim m_{max}$ which occurs at $T \sim 1.06 T_c$. This value is in qualitative agreement with the result obtained from the $L_{max} \sim a$ condition in the previous section. Unfortunately, this fall is much more rapid than the data, and the question arises what is the physical nature of states between 1.1-1.4 T_c for set 1 and 1.1-1.8 T_c for Set 2.

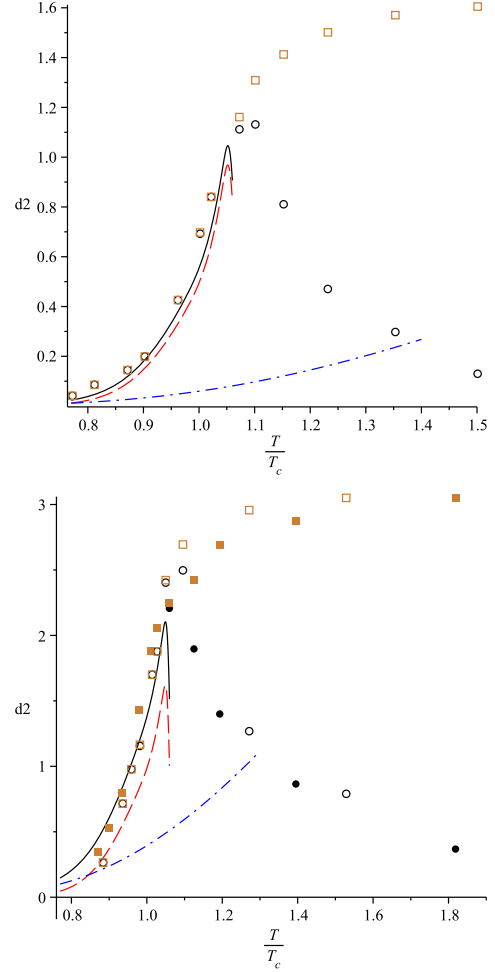


FIG. 6: (color online) Various contributions to the susceptibility $d_2(T)$ as a function of the temperature. The upper figure shows the lattice data of the Set 1 (2 flavors at $m_\pi = 770 \text{ MeV}$) from ref.[5], with quark contribution subtracted, are shown by (black) circles. The unsubtracted data are also included, as (brown) boxes for comparison.) The (red) dashed line corresponds to hybrid (or “stringy”) baryons. The (blue) dash-dotted line corresponds to the sum of the lowest 20-plet states. The (black) solid line is the overall baryonic contribution. The parameters used are $x = 0.62$ and $y = 0.08$. The lower plot is for Set 2 (2+1 flavors at $m_\pi = 220 \text{ MeV}$) [6]. The lattice data on susceptibility [6] with quark contribution subtracted are shown as black circles (solid ones for $N_\tau = 6$ and open ones for $N_\tau = 4$). The unsubtracted data are also included as brown boxes (solid ones for $N_\tau = 6$ and open ones for $N_\tau = 4$) for comparison. The parameters used are $x = 0.51$ and $y = 0.08$.

Those cannot be the “non-stringy” baryons, shown by the dash-dotted curves. First of all, their contribution have the wrong shape: it is increasing rather than decreasing. Furthermore, we terminated those lines at the melting temperature of baryons calculated in [8], modified for the particular quark masses used here. Note that

in all cases the melting temperature is reached before the lowest states contribution exceeds the lattice susceptibility.

The physical meaning of the factor x can be traced back to our choice of the density of states. Note we have used a simplified formula $\rho \sim e^S \sim 5x^{\frac{1}{a}}$ while the realistic Hagedorn model has $\rho \sim m^{-5/2}e^{\alpha m} \sim (\frac{1}{a})^{-5/2}5^{\frac{1}{a}}$. A crude estimate of x (in two flavors for example) can be made by identifying the two with $l = L_{max}$ and a taken from Fig.5. We obtain $x \doteq 1$ at $T = 0.8T_c$ and $x = 0.82$ at $T = 1.0T_c$.

V. CHIRAL DYNAMICS AND THE BARYONS

A. Why do we have two types of hadrons?

In a narrow sense, chiral dynamics is related to the dependence on the dynamical quark masses in the theory m_q when they are small or vanishing. In a more broad sense the issue includes an old question of to what extent the baryons are made of their “pion cloud”, and to what extent of quarks and confining strings, as in the nonrelativistic quark model. Hadronic physics has been oscillating between these two conflicting points of view for decades, with drastically different expectations for T and μ dependencies of hadronic masses following from them.

One extreme point of view, following from the Skyrme model and application of the QCD sum rules, suggested that hadronic masses are due to sigma/pion bags and are impossible without the chiral symmetry breaking and nonzero $\langle\bar{\psi}\psi\rangle$. If so, one would expect drastic changes or even vanishing of hadronic masses at the chiral restoration transitions [21].

The opposite point of view is that the sensitivity of baryon masses to chiral dynamics is restricted to explicit chirally odd coefficient of the quark mass, the sigma term. Here we will adhere to this conservative point of view.

Before turning to the chiral effect on the baryon mass and density of states, we want to point out a significant difference between (i) the lowest baryons (in each channel, such as N, Δ) and (ii) the bulk of hybrid baryons.

The former ones (i) – as experiment and lattice simulations told us – are strongly interacting with pions and chiral condensate. They do not have nearby parity partners. Significant part of their mass is believed to be related to “the pion cloud”, the extreme model on that is of course the Skyrme model which look at them as being pionic solitons. Instanton liquid model explains their masses well, using propagators based on instanton zero modes.

The latter (ii), the bulk of excited baryons, are on the contrary very insensitive to chiral physics. The most vivid spectroscopic evidence for that is parity doubling phenomenon, see extensive set of data on that in [22]. As was repeatedly emphasized in discussions of the matter, close pairs of opposite parity also imply weak coupling

to pions, which was also evident from the magnitude of decay matrix elements.

Why are these excited baryons behave like this? Our interpretation of them as “stringy” excitations would suggest that perhaps interaction of the color string and chiral condensate is small. This was in fact demonstrated on the lattice already 20 years ago [23]: in the vicinity of static quark the $\langle\bar{\psi}\psi\rangle$ is reduced by few percents only.

Instanton liquid model provides another interpretation of this phenomenon: it is a reflection of the Dirac spectrum in the field of an instanton, in which there is one (chiral) zero mode plus a continuum of non-chiral nonzero ones. The lowest hadrons are in this model viewed as exceptional states, built from collectivized zero modes, unlike all the excited states.

The lowest excitations are described via some potential models (especially accurate for heavy quarkonia) as radial and orbital excitation of moving quarks. Excitations in which quarks are basically at the same state as in the lowest hadrons but a *string* is excited are called “*hybrid states*”: there is vast lattice and experimental literature about them. The string-Hagedorn argument mentioned above implies, that such states are dominant at large excitations.

B. Chiral restoration transition and the lowest baryons

In the model proposed we assumed that the strongest sensitivity to small quark mass is entirely due to the “lowest” states with each quantum numbers. The mass of some baryonic state can be expressed by

$$m_B = m_q \langle B | \bar{\psi}\psi | B \rangle + \text{“gluonic part”} \quad (26)$$

where the coefficient of the quark mass is the scalar quark density: it is known as the sigma term.

In the calculation above we had fixed its magnitude from lattice works, in the vacuum: now is the time to discuss its dependence on the temperature. Following the idea that any chirally-odd quantity should disappear at chiral restoration transition, and furthermore that the sigma terms for any hadron is more or less proportional to the VEV or quark condensate, we propose to incorporate the chiral effect and μ dependence through the following formula:

$$m(T, \mu) = km_\pi^2 \frac{\langle B | \bar{\psi}\psi | B \rangle(T, \mu)}{\langle B | \bar{\psi}\psi | B \rangle|_{T=\mu=0}} + N_s m_s + \sigma_V(T) L(T) \quad (27)$$

In the absence of knowledge of the expectation value of $\bar{\psi}\psi$ with respect to the baryonic state, we simply assume normalized chiral condensate associated with some baryonic state is given by its counterpart in vacuum state:

$$\frac{\langle B | \bar{\psi}\psi | B \rangle(T, \mu)}{\langle B | \bar{\psi}\psi | B \rangle|_{T=\mu=0}} = \frac{\langle \bar{\psi}\psi \rangle(T, \mu)}{\langle \bar{\psi}\psi \rangle|_{T=\mu=0}} \quad (28)$$

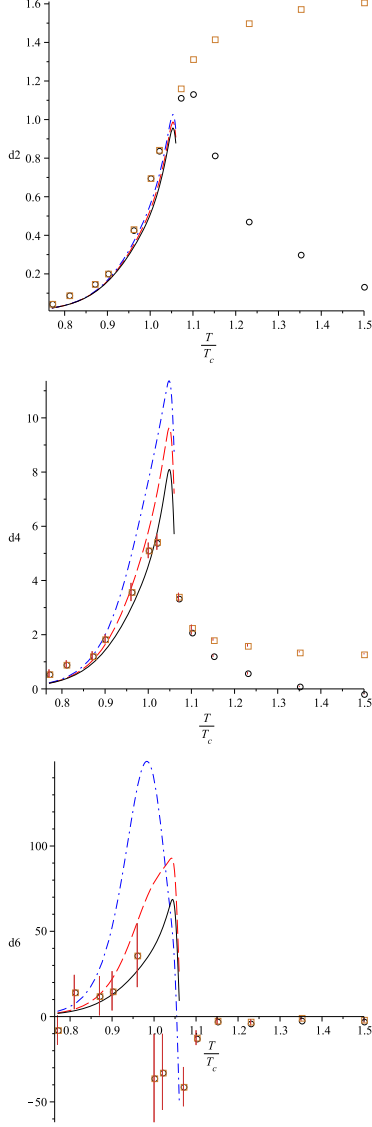


FIG. 7: (color online) Three figures display the temperature dependence of the second, fourth and sixth susceptibilities. The points are the Set 1 lattice data with the quark contribution subtracted. The lines correspond to the model discussed in the text, with μ dependent stringy and chiral baryons. The parameters used are $x = 0.6$, $y = 0.08$ and $\mu_c = \infty$ (black solid line), $\mu_c = 2T_c$ (red dashed line) and $\mu_c = 1.33T_c$ (blue dash-dotted line).

The temperature dependence has been measure on the lattice[24]. We fit the normalized chiral condensate by the following:

$$\frac{\langle \bar{\psi}\psi \rangle(T, \mu = 0)}{\langle \bar{\psi}\psi \rangle|_{T=\mu=0}} = 0.55 - 0.42 \tanh(9.47 \frac{T}{T_c} - 9.55) \quad (29)$$

The μ dependence enters quadratically by the $\mu \leftrightarrow -\mu$ symmetry, i.e. we use the collective coordinate $\sqrt{(T/T_c)^2 + (\mu/\mu_c)^2}$ instead of T/T_c . Similar

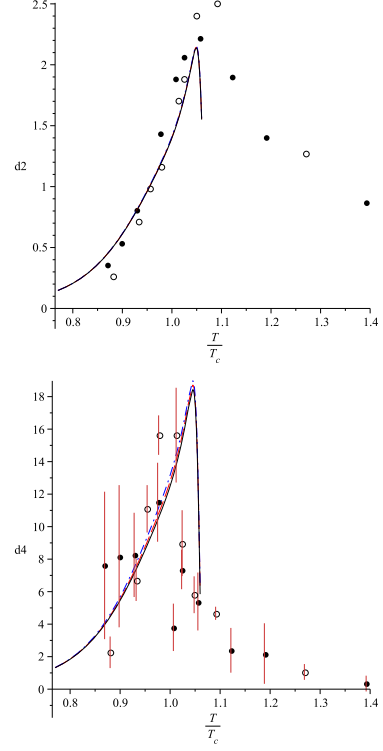


FIG. 8: (color online) The temperature dependence of the second and fourth susceptibilities, for Set 2 lattice data, with the quark contribution subtracted. The (black) solid circles correspond to $N_\tau = 6$ and open circles to $N_\tau = 4$. The curves are for the model described in the text, with parameters values equal to $x = 0.51$, $y = 0.08$ and $\mu_c = \infty$ (black solid line), $\mu_c = 2T_c$ (red dashed line) and $\mu_c = 1.33T_c$ (blue dash-dotted line).

parametrization is also used in [7]. We leave μ_c as a free parameter. With chiral effect incorporating both T and μ dependence, we are ready to calculate the susceptibility using (25). Since μ appears in many places in (24), taking derivatives becomes cumbersome. We simply use numerical differentiation method. Further simplification can be made by noting the evenness of (24) as a function of μ/T . $2n$ -th derivative with respect to μ/T amounts to n -th derivative with respect to $(\mu/T)^2$.

As already discussed in [7, 25], in the model of baryon gas the deviations of d_4/d_2 from 9 follows from the fact that their masses are effectively dependent on μ . In our string model, this appears as a μ dependent density of states $\rho(T, \mu)$ [32].

We show the effect of μ dependence of baryon mass in Fig.7(Set 1) and Fig.8(Set 2). We see the inclusion of this effect hardly change the d_2 plot, but shifts the peak upwards in d_4 and d_6 plots. Smaller value of μ_c results in higher peak. However the peaks of d_4 and d_6 are over predicted either with ($\mu_c = 1.33, 2T_c$) or without ($\mu_c = \infty$) μ dependence of the baryon mass. The shift of the peak

is more prominent near T_c , where the chiral condensate drops rapidly, thus the masses of the lowest states change rapidly as well. It is also worth noting that the shift is less prominent in case of 2+1 flavors model. This is because in that case a smaller fraction of the mass has changed due to a smaller sigma term.

It is also instructive to plot the kurtosis from our stringy baryon model. We show the plot of kurtosis both with and without the chiral effect in Fig.9. A sharp dropping of the kurtosis is observed near the critical temperature. However the limitation of the model prevents us to go beyond $1.06T_c$, where the kurtosis is supposed to drop to 1. The importance of μ dependence of the baryon mass is clearly illustrated in Fig.9. Without the μ dependent density of states, the drop is a simple vertical fall, while the inclusion of chiral effect produces a bump where the chiral condensate drops rapidly. The bump is more prominent for 2 flavors Set 1, in which case the lowest states have relative large fraction of mass that is chirally sensitive.

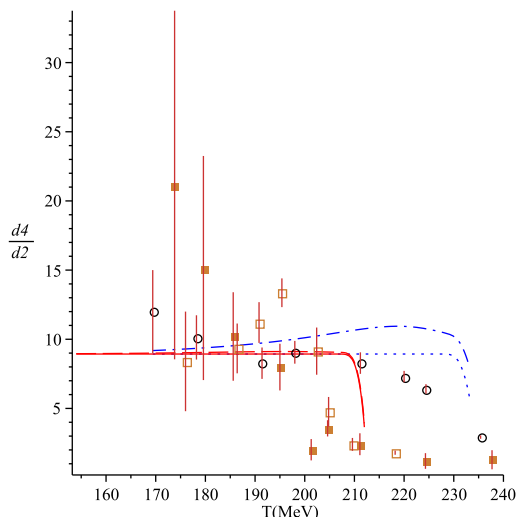


FIG. 9: (color online) The temperature dependence of the kurtosis $\frac{d4}{d2}$. All discussed lattice data are shown here: Set 1 (2 flavor at $m_\pi = 770 \text{ MeV}$) by (blue) circles, Set 2 (2+1 flavor at $m_\pi = 220 \text{ MeV}$) by (red) solid boxes and open boxes, for $N_\tau = 6$ and $N_\tau = 4$ respectively. Four curves in the plot are for 2 flavor at $m_\pi = 770 \text{ MeV}$ without (blue dotted) and with (blue dash-dotted) chiral effect, 2+1 flavor at $m_\pi = 220 \text{ MeV}$ without (red solid) and with (red dashed) chiral effect. The same parameters are used as in Fig.6,7,8. In particular, we have chosen $\mu_c = 2T_c$ for cases with chiral effect)

The sign and magnitude of the chiral restoration effect in our model is in sharp contrast with the PQM model [26], predicting sharp and very large deviation of the kurtosis from 9, up to about 15. That happened because in Brown-Rho-type dropping of hadronic masses

prior to chiral restoration transition. In Fig.9 there is certain mixed signal here: Set 2 data at $N_\tau = 4$ and $N_\tau = 6$ show somewhat different trend. Unfortunately current data are still insufficient to make clear distinction between our conservative approach (only the sigma terms melt at chiral restoration) and the Brown-Rho behavior. We hope this interesting issues will be clarified in the future.

VI. DISCUSSION

A. Quarks bound to monopoles?

As we have already emphasized above, lattice data on the deconfinement transition give rather different width of the transition region for baryons (discussed in the preceding section) and the quarks. While the baryons show rapid rise and then rapid fall already at about $1.05T_c$, quark suppression is dominated by the Polyakov loop, which only goes to 1 at $2T_c$. Such mismatch of the widths, be nearly and order of magnitude, leave some “hole” in the middle: indeed, one can see from Fig.7 that our model has certain deficit at $T = (1.1 - 1.4)T_c$, as compared to the lattice data. So, it can be a deficiency of the model, or some missing component.

Thinking about possible missing states leads us to propose one idea, which is by itself well known in theoretical literature, yet (for our knowledge) never been used in QCD thermodynamics context so far. Static monopole solution has 3-dimensional fermionic zero mode. It is important to note, that its existence follows from topological theorems and thus does not depend on details of the monopole profile. In particular, it exists whether monopole can or cannot be described semiclassically.

In vacuum $T = 0$ this simply means that a quark can be bound to the monopole. For a massless quark in vacuum there are two degenerate states, with fermionic numbers 1 and 0[33]. For N_f quark flavors each can be either present or absent, leading to 2^{N_f} states.

Euclidean finite T formalism breaks the degeneracy of this situation: the bosonic objects should have periodic wave function, and thus time-independence is unaffected, while fermionic objects should have antiperiodic wave functions in Euclidean time. Thus one should inevitably introduce $\exp(iE\tau)$ with the lowest odd Matsubara frequencies $E = \pm\pi T$ into the fermionic wave function, making the composite fermionic magnetic object heavier

$$M_{fm} \approx M_{mono} + \pi T \quad (30)$$

The mass of the monopole is believed to be minimal at T_c , while its value is not yet measured. It has been argued from BEC condition [27] that it may be as small as $M_{mono} \sim 200 \text{ MeV}$: if so, the minimal mass of the composite object is about $M_{fm}(T = T_c) \sim .8 \text{ GeV}$, which is accidentally close to lattice data on quark quasiparti-

cles. Note however, that such composite has only *one* spin state.

At temperatures $T \sim T_c$, the monopoles remain strongly correlated and behaves as liquid[28], preventing us using ideal gas formula. While the density is measured in $SU(2)$ gauge theory on the lattice[29]. The scaled monopole density is parametrized by:

$$\frac{n}{T^3} = \frac{A}{\ln^2(\frac{T}{\Lambda})} \quad (31)$$

$$\text{with } A = 0.557 \frac{T_c}{\Lambda} = 2.69 \quad (32)$$

The density of monopole(anti-monopole)-zero mode bound state is estimated as $ne^{-\pi}$. The additional Boltzmann factor arises from the Matsubara frequency. We plot the bound state contribution in Fig.10. Taking into account a very schematic model and preliminary data on the monopole density, we conclude that magnetic composite fermions do have a potential to be the “missing ingredient” mentioned at the beginning of this section. Of course, to know it for sure much more work is needed. In particular, existence of such composite fermions with a magnetic charge can be investigated on the lattice, by observing the correlations between the monopole paths and the fermionic operators (especially the fermionic spin).

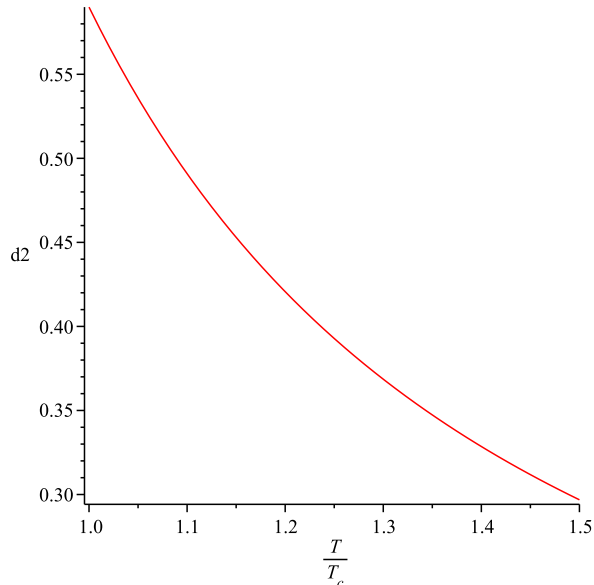


FIG. 10: The contribution from monopole(antimonopole)-zero mode bound state. We have used a degeneracy factor $2N_c N_f$ since the zero mode only has one spin

B. Outlook

We hope that multiple details of the last sections have not detracted the reader from the main ideas of the model, which are (i) exponential rise of the stringy partition function near T_c , as well as (ii) the upper cutoff of the strings length defined by the quark density. Those two phenomena are the basis for “the rise and fall of the baryons” put into the title.

Our conservative treatment of the chiral dynamics seems to be working. The dependence of the baryon masses on m_q , light quark bare mass, and related effects due to chiral symmetry restoration and vanishing of the “pion cloud” are small but interesting corrections to the main picture. We have tried – using lattice data whenever those are available – to parametrize those effects and include them into the model, in the last few sections. The reader may at this point ask what is actually achieved by doing this.

Any model is as good as ideas put into it, and in order to test it one can see if it has any predictive power. By this we mean its application to wide range of the QCD-like theories. So far we considered two directions: (i) variable light quark mass, and (ii) increasing μ/T or – which is basically the same – including the susceptibilities with more derivatives.

We suggest to address the same issues using other theories, especially with dynamical *adjoint* fermions. In this case the critical points of the deconfinement transition and that of chiral restoration are very different

$$T_{deconfinement} \ll T_{chiral} \quad (33)$$

so that there is a new intermediate phase, that of “deconfined constituent quarks”. For three colors the deconfinement is in this case the first order transition, while the chiral one is of the second order, see e.g. [30] and references for earlier papers therein. Another reason one may be interested in this direction is possible relation to supersymmetric theories.

For simplicity and continuity of the observables, one may introduce non-dynamical fundamental quarks which would have their own chemical potential and form baryons with the usual quantum numbers, basically repeating the same analysis as was done for Set.1 and 2 we used, but with a different ensemble of gauge fields, now with some dynamical adjoint fermions. In this case one expect to find the “rise and fall” of the stringy baryons be seen at the deconfinement transition, while the effects related with chiral condensate (and sigma term) melting occurring at completely different chiral restoration temperature. Large intermediate phase would be a great place to finally find out whether confinement is or is not required for the existence of the “chiral” baryons. Another difference between adjoint and fundamental fermions is a different number of fermionic zero modes of monopoles/dyons: there are *two* bound states of adjoint fermions rather than one. So, if such states

play role above the deconfinement, they should be significantly more important in the adjoint theories, especially with more than one fermion flavors.

Appendix

In this appendix we collected some information we used from different lattice works, to parametrize several quantities of interest.

The Polyakov loop in two flavors QCD is shown in Fig.11. It reaches 1 at around $2.5T_c$, where the quark density reduces to the free quark situation. The Polyakov loop is parametrized by:

$$\langle L(T) \rangle = \begin{cases} 0.038 + 5.20(T - 0.77)^{2.24} & T < 1.07T_c \\ -0.164 + 1.048(T - 1.0)^{0.242} & T > 1.07T_c \end{cases} \quad (34)$$

The thermal quark mass as a function of the temperature is shown in Fig.12. The thermal quark mass m_q around the critical temperature is important as it affects the cutoff in the baryon density of states via n_q . Recent lattice measurement[31] indicated $m_q/T \sim 0.8$ in temperature range $T \sim 1.25 - 3T_c$. Thermal mass below $1.25T_c$ is still not known. In the absence of additional data, we estimate the quark thermal mass as half of the internal energy for quark-antiquark at infinity separation U_∞ . The data of U_∞ are taken from Table I of [16][34]. The thermal mass of the quarks are fitted with:

$$\frac{m_q}{T_c} = 6.12 - 4.76 \tanh(12.38 \frac{T}{T_c} - 13.16) \quad (35)$$

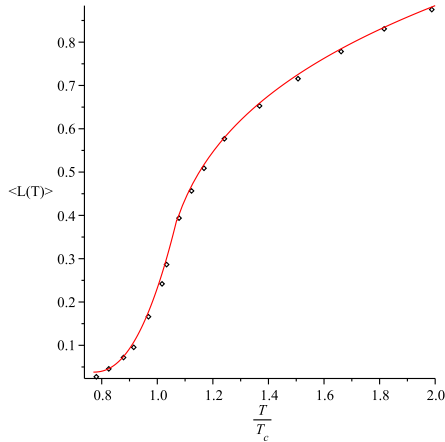


FIG. 11: (Color online) The points are lattice data on the temperature dependence of the Polyakov loop from Ref.[15], fitted with the expression (34)

The chiral condensate from the lattice measurement (29). is shown In Fig.13. It is defined as,

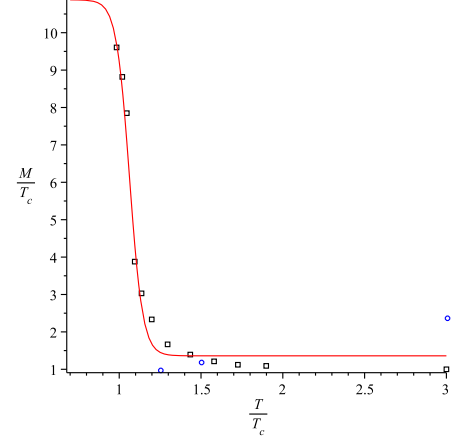


FIG. 12: (Color online) The points are lattice data on the temperature dependence of the effective quark mass, deduced from the potentials studied in Ref.[16]. The (red) line is a fit with expression (35). Direct measurements of the quark effective mass from the dispersion relations of the quark quasi-particles for two temperatures, $T = 1.25T_c, 1.5T_c, 3T_c$, from Ref.[31] are shown by (blue) circles for comparison.

$\frac{\langle \bar{\psi}\psi \rangle_{l,T} - \frac{m_l}{m_s} \langle \bar{\psi}\psi \rangle_{s,T}}{\langle \bar{\psi}\psi \rangle_{l,0} - \frac{m_l}{m_s} \langle \bar{\psi}\psi \rangle_{s,0}}$ and measure at finite mass ratio of light and strange quark $\frac{m_l}{m_s}$. We will however use this value as our normalized chiral condensate, which is valid at $\frac{m_l}{m_s} \rightarrow 0$

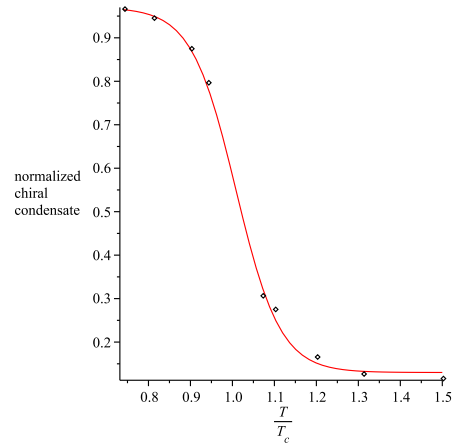


FIG. 13: (Color online) The temperature dependence of the chiral condensate, normalized to its vacuum value. The (black) dots are taken from lattice work Ref.[24] and fitted with the red curve according to expression (29).

We fix the μ dependence by the following ansatz:

by the US-DOE grants DE-FG02-88ER40388 and DE-FG03-97ER4014.

$$\frac{\langle\bar{\psi}\psi\rangle(T,\mu)}{\langle\bar{\psi}\psi\rangle|_{T=\mu=0}} = 0.55 - 0.42 \tanh(9.47\sqrt{(T/T_c)^2 + (\mu/\mu_c)^2} - 9.55) \quad (36)$$

Acknowledgments

We thank Jinfeng Liao, Chuan Miao and Claudia Ratti for helpful discussions. Our work was partially supported

-
- [1] F. Karsch, K. Redlich and A. Tawfik, Phys. Lett. B **571**, 67 (2003) [arXiv:hep-ph/0306208].
 - [2] R. Hagedorn, Nuovo Cim. Suppl. **3**, 147 (1965).
 - [3] E. V. Shuryak, Phys. Rept. **61**, 71 (1980).
 - [4] E. Shuryak, arXiv:0903.3734 [nucl-th].
 - [5] C. R. Allton *et al.*, Phys. Rev. D **71**, 054508 (2005) [arXiv:hep-lat/0501030].
 - [6] M. Cheng *et al.*, Phys. Rev. D **79**, 074505 (2009) [arXiv:0811.1006 [hep-lat]].
 - [7] J. Liao and E. V. Shuryak, Phys. Rev. D **73**, 014509 (2006) [arXiv:hep-ph/0510110].
 - [8] J. Liao and E. V. Shuryak, Nucl. Phys. A **775**, 224 (2006) [arXiv:hep-ph/0508035].
 - [9] C. Ratti, M. A. Thaler and W. Weise, Phys. Rev. D **73**, 014019 (2006) [arXiv:hep-ph/0506234].
 - [10] S. Roessner, C. Ratti and W. Weise, Phys. Rev. D **75**, 034007 (2007) [arXiv:hep-ph/0609281].
 - [11] C. Ratti, S. Roessner and W. Weise, Phys. Lett. B **649**, 57 (2007) [arXiv:hep-ph/0701091].
 - [12] B. Bringoltz and M. Teper, Phys. Rev. D **73**, 014517 (2006) [arXiv:hep-lat/0508021].
 - [13] G. S. Bali, arXiv:hep-ph/9809351.
 - [14] G. S. Bali, T. Dussel, T. Lippert, H. Neff, Z. Prkacin and K. Schilling, Nucl. Phys. Proc. Suppl. **153**, 9 (2006) [arXiv:hep-lat/0512018].
 - [15] O. Kaczmarek and F. Zantow, Phys. Rev. D **71**, 114510 (2005) [arXiv:hep-lat/0503017].
 - [16] O. Kaczmarek and F. Zantow, arXiv:hep-lat/0506019.
 - [17] F. X. Lee, “Excited baryon spectrum from lattice QCD,”
 - [18] C. Amsler *et al.* [Particle Data Group], Phys. Lett. B **667**, 1 (2008).
 - [19] F. Karsch, E. Laermann and A. Peikert, Nucl. Phys. B **605**, 579 (2001) [arXiv:hep-lat/0012023].
 - [20] M. Cheng *et al.*, Phys. Rev. D **77**, 014511 (2008) [arXiv:0710.0354 [hep-lat]].
 - [21] G. E. Brown and M. Rho, Phys. Rept. **363**, 85 (2002) [arXiv:hep-ph/0103102].
 - [22] L. Y. Glozman, Phys. Rev. Lett. **99**, 191602 (2007) [arXiv:0706.3288 [hep-ph]].
 - [23] W. Feilmair, M. Faber and H. Markum, Phys. Lett. B **221**, 363 (1989).
 - [24] A. Bazavov *et al.*, Phys. Rev. D **80**, 014504 (2009) [arXiv:0903.4379 [hep-lat]].
 - [25] F. Karsch, S. Ejiri and K. Redlich, Nucl. Phys. A **774**, 619 (2006) [arXiv:hep-ph/0510126].
 - [26] B. Stokic, B. Friman and K. Redlich, Phys. Lett. B **673**, 192 (2009) [arXiv:0809.3129 [hep-ph]].
 - [27] M. Cristoforetti and E. Shuryak, arXiv:0906.2019 [hep-ph].
 - [28] J. Liao and E. Shuryak, Phys. Rev. Lett. **101**, 162302 (2008) [arXiv:0804.0255 [hep-ph]].
 - [29] A. D’Alessandro and M. D’Elia, Nucl. Phys. B **799**, 241 (2008) [arXiv:0711.1266 [hep-lat]].
 - [30] G. Cossu, M. D’Elia, A. Di Giacomo, G. Lacagnina and C. Pica, Phys. Rev. D **77**, 074506 (2008) [arXiv:0802.1795 [hep-lat]].
 - [31] F. Karsch and M. Kitazawa, arXiv:0906.3941 [hep-lat].
 - [32] We of course also have μ dependence in the mass upper cutoff of the hybrid states, but it only causes small deviation
 - [33] in the context of $SU(2)$ supersymmetric model those are sometimes redefined and called states with fermionic number 1/2 and -1/2: but we would not do so. Finite temperature breaks the supersymmetry anyway.
 - [34] We use data only at temperature above the critical value. Below the critical temperature, half of U_∞ gives the meson mass, and thermal quark mass is not important due to Polyakov loop suppression